

# Ultrasonic Flowmeter for Accurately Measuring Flare Gas over a Wide Velocity Range

Lei Sui\*, Toan H. Nguyen, James E. Matson, Peter Espina and IvanTew

GE—Sensing and Inspection Technologies  
1100 Technology Park Dr., Billerica, MA 01821 USA

\*Tel: 978-437-1664

\*Email: [lei.sui@ge.com](mailto:lei.sui@ge.com)

**Abstract:** Flare gas ultrasonic flow measurement has now been well established with more than 3000 units installed worldwide in process plants and refineries. One of the remaining technical challenges in flare gas ultrasonic flowmetering is to deal with extremely high flare flows (greater than 80 m/s) during emergency flaring. High flare flows introduce soaring flow noise, cause ultrasonic beam drift and thus deteriorate ultrasonic signal quality, leading to an ultimate failure of the flare gas flow measurement. In this paper, the ultrasonic propagation in flare gas has been studied, the beam drift due to gas flow has been investigated and improvements from both mechanical and transducer perspectives have been made. An improved flare gas ultrasonic flow meter has been developed to demonstrate the accurate measurement of air flow up to 123.7 m/s. Testing data have been presented for two typical configurations, Bias 90 and Diagonal 45, in comparison with a Venturi reference meter. The overall accuracy of the new flare meter is demonstrated to be 3-4%, and the relative standard deviation of the meter readings is within 1.2%. This new development could translate into higher flow-velocity flare gas measurement and monitoring, depending on the flare gas composition in an actual application.

**Keywords:** Ultrasonic flowmeter, Flare gas, Beam drift

## 1. Introduction:

Flare systems are primarily installed for safety purposes in chemical, petrochemical, refining, and other plants. These flare systems are used to vent and burn off hydrocarbons and other unwanted gases under routine and emergency conditions, such as an unexpected shutdown. Today, it has become an international awareness to measure and monitor flare gas flow for both environmental and economical reasons <sup>[1][2][3]</sup>. The measurement of flare gas helps to comply with environmental regulations, identify points of leakage, and reconcile plant mass balance.

Regardless of its importance and high demand, flare gas flow measurement itself is challenging mainly due to factors such as: unsteady flow velocity, pressure fluctuations, aggressive chemicals in the gas, potential high temperature excursions and a wide-range of flow rates encountered. In particular, it requires instrumentation to be capable of measuring gas flow over a wide range of velocities: from 0.03 m/s under lowest flow conditions, through 0.15-0.5 m/s for most normal operations, up to 80 m/s or above during emergency flaring. Traditional flowmeters based on differential pressure, thermal-mass and vortex shedding have been explored for flare gas application, but their individual success has been limited due to reasons such as, restricted rangeability (turndown ratio), inability to handle unsteady flows, corrosion, and sensitivity to changes in gas composition.

In the early 1980s, a flare gas ultrasonic flowmeter was first jointly developed by Panametrics (now GE Enterprise Solutions—Sensing) and Exxon (now Exxon Mobil) in Baytown, Texas, USA, demonstrating great success<sup>[1]</sup>. Since then, ultrasonic flowmeters have been gaining more and more popularity for flare gas measurement, mainly because of its high turndown ratio, its relatively low installation and maintenance costs, its capability of handling unsteady flows, and its independence on gas composition. Today, ultrasonic flowmetering is the accepted technology for monitoring flare gas, with more than 3,000 installations worldwide.

Although flare gas ultrasonic flowmeters have evolved with many improvements over the past 25 years, one of the remaining technical challenges is to deal with extremely high flow velocity up to 80 m/s and above. Such high flare gas flows can occur during a process shutdown when all the process gases need to be flared. It is difficult to apply ultrasonic flowmeters to measuring extremely high-velocity flare gas flow largely because ultrasonic signal quality deteriorates quickly with flow rate. The poor signal quality at high flow velocities, usually quantified by low signal-to-noise ratio (SNR), is due to such factors as beam drift induced by high-velocity flow, greatly-increased noise level associated with high-flow velocities, and turbulence-related attenuation, scattering and distortion of ultrasonic signals<sup>[4]</sup>. As a result, flare gas ultrasonic flowmeters available on the market today offer the maximum velocity capability of 85 m/s – 100 m/s<sup>[5][6]</sup>.

In this paper, an ultrasonic flowmeter has been developed and tested for high-velocity gas measurement up to 123.7 m/s in air. Some of the enabling technologies behind this new development are detailed, including proper design of transducer dimension, transducer separation and operating frequency, and the implementation of recovery angle to the downstream transducer only. Testing results obtained from a wind tunnel in the Energy and Propulsion Technologies Laboratory at the GE Global Research Center located in Niskayuna, NY are presented and compared with a reference meter, which has an uncertainty of 1-2%, depending on the flow velocity range (refer to Appendix for details). The accuracy of our new meter is demonstrated to be better than 3-4% with reference meter uncertainty included, and the relative standard deviation of the new meter is within 1.2%.

## 2. Methodology

### 2.1. Transducer Dimension, Separation, and Frequency

Using ultrasound to measure flow velocity has been a well-known technique for decades<sup>[7]</sup>. Over the years, many different types of ultrasonic flowmeters have been developed—the operating principle varies from transit-time to Doppler and to Transflexion<sup>[8]</sup>. Among these, transit-time based ultrasonic flow measurement has become the most popular method thanks to its superior accuracy and robustness.

Transit-time ultrasonic flowmeters take advantage of a simple principle, called “time of flight”, as illustrated in Fig. 1. Specifically, the time it takes for an ultrasonic signal to travel against the flow (i.e., upstream),  $t_{up}$ , is longer than that it takes following the flow (i.e., downstream),  $t_{dn}$ . The difference between upstream and downstream traveling times,  $\Delta t$ , is directly proportional to the flow velocity as follows<sup>[8][9]</sup>:

$$V = \frac{P}{2 \cos \theta} \left( \frac{1}{t_{dn}} - \frac{1}{t_{up}} \right) = \frac{P}{2 \cos \theta} \left( \frac{\Delta t}{t_{dn} t_{up}} \right), \quad (1)$$

where  $V$  is the flow velocity to be measured,  $P$  is the ultrasonic path length, and  $\theta$  is the acute angle between the ultrasonic path and the axis of the flowcell or pipe section.

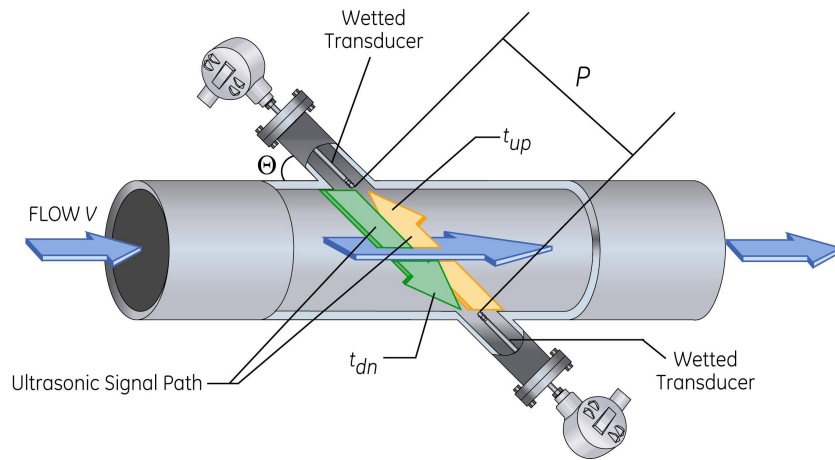


Fig. 1 The operating principle of a transit-time based ultrasonic flowmeter.

From Eq. (1), it can be seen that the operation of an ultrasonic flowmeter strongly depends on the timing of  $t_{up}$ ,  $t_{dn}$ , and  $\Delta t$ . The measurements of  $t_{up}$ ,  $t_{dn}$ , and  $\Delta t$  conversely rely on the quality of the received ultrasonic signal, i.e., signal-to-noise ratio (SNR). Therefore, it is important to understand how the ultrasonic signal generated by an ultrasonic transducer is propagating in a gas medium towards the receiving transducer.

For linear ultrasound propagation, there exist near-field and far-field regions, with the latter beginning at the so-called Rayleigh distance <sup>[10]</sup>. The near field is characterized by wavefronts that are approximately planar, and the far field is characterized by wavefronts that are spherical. In the case where an ultrasonic wave (characterized by its frequency  $f$  or by its wavelength  $\lambda$ ) propagates from a circular transducer with a radius of  $a$ , as schematically illustrated in Fig. 2, Rayleigh distance,  $L_R$ , is defined as follows:

$$L_R = \frac{1}{2}ka^2 = \pi \frac{a^2}{\lambda}, \quad (2)$$

where  $k = \frac{2\pi f}{c}$  is the wave number, and  $c$  is the speed of sound in the medium.

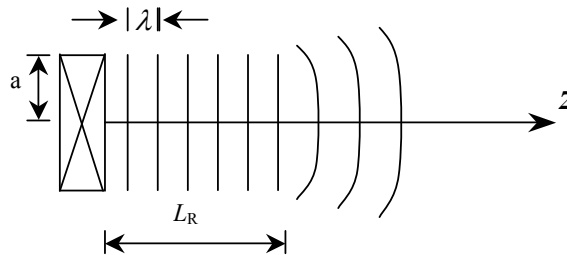


Fig. 2 Ultrasound propagation in a medium across both near field and far field, nominally separated by Rayleigh Distance,  $L_R$ .

In the far field, the pressure amplitude at location  $z$  (which is measured along the transducer axis with  $z = 0$  starting at the transducer surface),  $P(z)$ , can be approximately written as <sup>[11]</sup>:

$$P(z) = K_0 \frac{a^2}{z} e^{-\alpha z}, \quad (3)$$

where  $K_0$  is a constant determined by the driving amplitude of the transducer, efficiency of the transducer, and the medium in which ultrasound is propagating, and  $\alpha$  is the ultrasonic attenuation coefficient in units of neper/m or dB/m. The ultrasonic attenuation coefficient depends on the medium in question and is typically a function of ultrasonic frequency in many fluids including air following the power law as:

$$\alpha = \alpha_0 f^n, \quad (4)$$

in which  $\alpha_0$  and  $n$  are two coefficients used to describe this function. In practice, both  $\alpha_0$  and  $n$  could be obtained by measuring ultrasound pressure at different frequencies and distances. For example, in air, ultrasonic attenuation coefficient could be a linear function of ultrasonic frequency, i.e.,  $n = 1$ , within the frequency range of 50–300 kHz <sup>[12]</sup>.

Substituting Eq. (4) into Eq. (3), we obtain:

$$P(z) = K_0 \frac{a^2}{z} e^{-\alpha_0 f^n z}. \quad (5)$$

In the context of flare gas application, Eq. (5) indicates that, in order to boost the ultrasonic signal amplitude, it is desirable to have transducers with a large radius (or diameter), to keep the separation of the transducer pair close, and to select a relatively low ultrasonic frequency. In reality, the transducer dimensions are limited by the cost of the transducers, the mechanical arrangement associated with the transducers, and the openings in the flowcell; the larger openings on the pipe tend to disturb the local flow profile, making it difficult to obtain accurate flow measurements. Similarly, the separation of the transducers is restricted by the accuracy requirement at low flowrates, where  $P$  should be larger than  $\frac{c^2}{2V \cos \theta} \Delta(\Delta t)$  in which  $\Delta(\Delta t)$  is the resolution of  $\Delta t$  primarily determined by the meter electronics and its signal processing; nanosecond resolution of  $\Delta t$  can be achieved with modern electronics and signal processing. In addition, the separation of the transducer pair should be larger than the Rayleigh distance, to avoid the near field interference effect <sup>[11]</sup>. Finally, the selection of an ultrasonic frequency is a trade-off between maximizing resolution and minimizing attenuation. Taking the above compromises into consideration, we have designed our transducers with a radius of 0.375" and a frequency of 100 kHz (refer to [13] for more transducer details), and chosen a separation of the transducer pair of ~6.5".

## 2.2. Recovery Angle

One particular difficulty with ultrasonic measurement of flare gas arises from the ultrasonic beam drift due to high velocity flows. In other words, ultrasonic signal will be blown away by the high-velocity flows; this flow carrying effect will result in a miss of the "perfectly aligned" targeted receiving transducer. The downstream ultrasonic beam drift and upstream ultrasonic beam drift due to flows are schematically illustrated in Fig. 3 (a) and (b), respectively. Based on simple vector addition, we can calculate the downstream beam drift angle  $\gamma$  due to flow velocity  $V$  in a gas medium characterized by its speed of sound  $c$  as follows (simple trigonometry-based vector addition has been omitted for clarity):

$$\gamma = \theta - \arctan\left(\frac{c \sin \theta}{c \cos \theta + V}\right) = \theta - \arctan\left(\frac{\sin \theta}{\cos \theta + M}\right), \quad (6)$$

where  $\theta$  is as defined above, i.e., the acute angle between the ultrasonic propagation and flow directions, and  $M = V/c$  is the Mach number. For beam drift angle calculations throughout this paper, the “counterclockwise” direction is referred to be the positive direction, and “clockwise” negative. Similarly, the upstream beam drift angle  $\gamma$  can be derived as follows:

$$\gamma = \begin{cases} \theta - \arctan\left(\frac{\sin \theta}{\cos \theta - M}\right) & \text{for } M < \cos \theta \\ \theta - 90^\circ & \text{for } M = \cos \theta \\ \theta - \arctan\left(\frac{\sin \theta}{\cos \theta - M}\right) - 180^\circ & \text{for } M > \cos \theta \end{cases}. \quad (7)$$

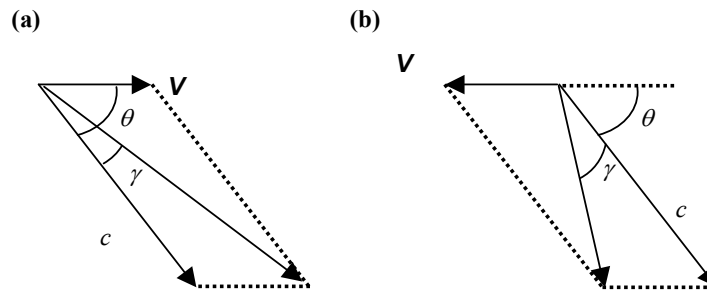


Fig. 3 Schematic illustration of the downstream ultrasonic beam drift effect (a) and the upstream ultrasonic beam drift effect (b) due to flow.

As can be seen from Eqs. (6) and (7), beam drift angle depends on ultrasonic path angle of  $\theta$  and Mach number (or the flow velocity for a medium with a given speed of sound). Fig. 4 (a) and (b) show the downstream and upstream beam drift angles, respectively, as a function of  $\theta$  at different Mach numbers. As shown, for a given flow of fluid or gas, typically, the greater the flow velocity is, the larger the absolute value of the beam drift angle is. In other words, as expected, a greater flow velocity normally translates into a more severe beam drift. However, an ultrasonic path angle  $\theta$  can be properly chosen to minimize the beam drift angle to some extent; generally the smaller the ultrasonic path angle, the smaller the absolute beam drift angle. In reality, the ultrasonic path angle is restricted by other considerations, such as mechanical arrangement, and low flow measurement accuracy requirement, where  $V \approx \frac{c^2}{2P \cos \theta} \Delta t$  (For example, a large ultrasonic path angle close to  $90^\circ$  would result in a larger inaccuracy; to the extreme, a path angle of  $90^\circ$  always leads to zero  $\Delta t$  and therefore no ultrasonic flowmeter can be made out of an ultrasonic path angle of  $90^\circ$ ). The ultrasonic path angle between  $30^\circ$  and  $60^\circ$  is most common in practice.

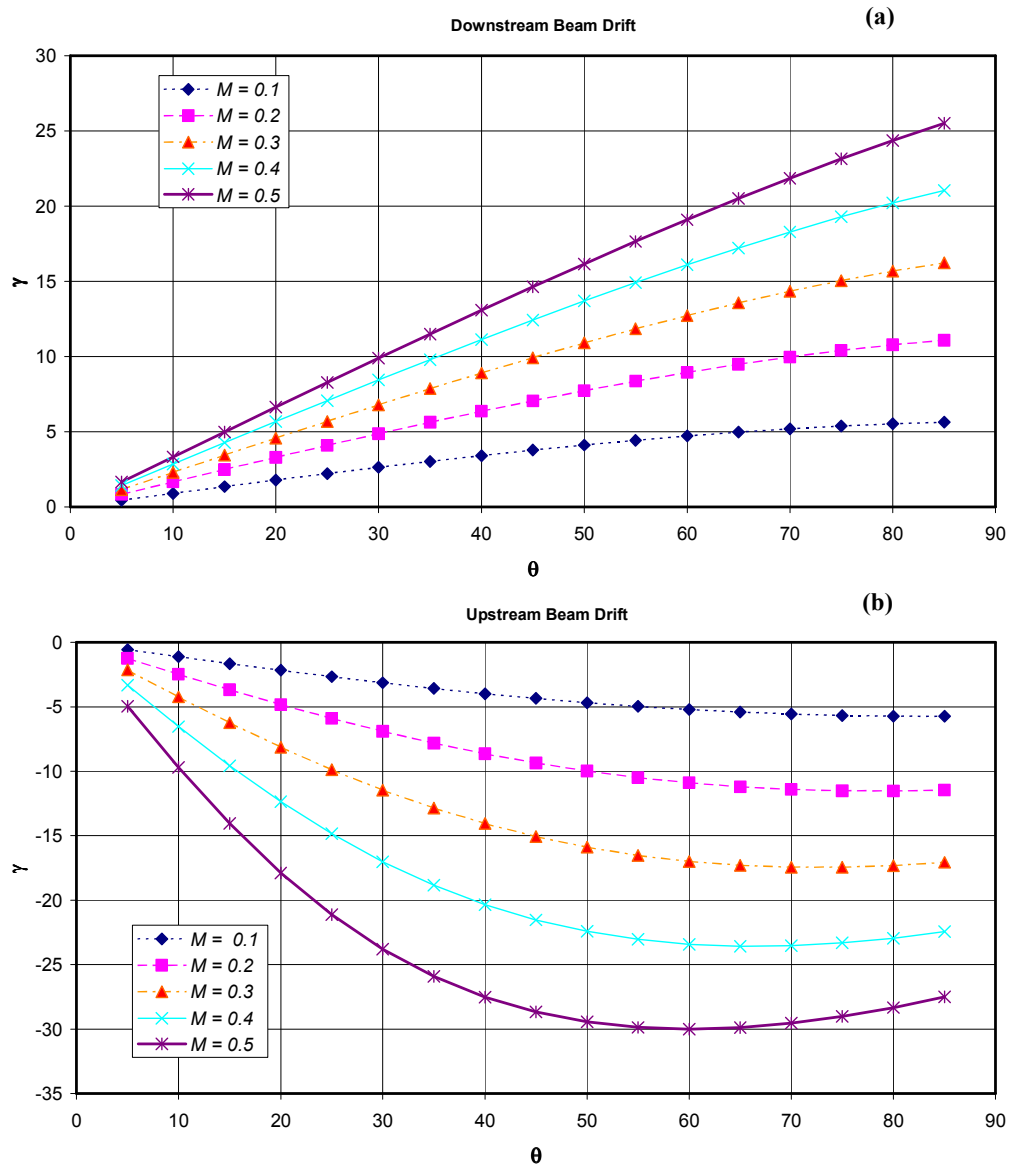


Fig. 4 (a) Downstream ultrasonic beam drift angle as a function of ultrasonic path angle at different Mach numbers; (b) Upstream ultrasonic beam drift angle as a function of ultrasonic path angle at different Mach numbers.

It should be noted, from Fig. 4 (a) and Fig. 4 (b), that the upstream ultrasonic beam drift is typically more severe than the downstream beam drift, for the same given flow. Simply put, for the same Mach number, the absolute upstream beam drift angle is larger than the downstream beam drift angle. For example, at Mach number  $M=0.3$  and  $\theta = 45^\circ$  (this could be a typical configuration for measuring high-flow flare gas), the upstream beam drift angle is about  $15.1^\circ$  while the downstream beam drift angle is about  $9.9^\circ$ . On one hand, this implies that the same high velocity flow causes more problems on the upstream signal than it does on the downstream signal. In fact, the systematic signal processing of a flare ultrasonic flowmeter is eventually limited by the upstream signal when it comes to measuring extremely high flows<sup>[4]</sup>. On the other hand, the above exemplary case reveals that the beam drift angle at high flows is not trivial. To

put this into context, the beam divergence angle,  $\phi$ , of a transducer with radius  $a$  (defined from centerline of the transducer to point where signal is at half strength) is given as follows <sup>[14]</sup>:

$$\sin \phi = 0.6 \frac{\lambda}{a} = 0.6 \frac{c}{f a}, \quad (8)$$

where  $\lambda$ ,  $f$  and  $c$  are the ultrasonic wavelength, frequency and velocity in the medium, respectively. In air, this angle of  $\phi$  is about  $12^\circ$  for an 100-kHz ultrasonic transducer with a radius of 0.375". For this transducer, the upstream signal is decreased by about 6 dB due to the beam drift alone at a flow of around 100 m/s in air, not to mention the other adverse effects imposed by the high flow, such as high flow noise and Doppler shift <sup>[15]</sup>.

Recovery angle can be implemented to offset or alleviate the aforementioned beam drift effect, as demonstrated in Reference [5], where recovery angles were applied to both downstream and upstream transducers. It should be noted that the accurate implementation of recovery angle on both transducers could be either time consuming, particularly in the field during the hot/cold tap procedures, or costly, or both. Since the above calculation of beam drift shows that the "bottleneck" of the operation of an ultrasonic flowmeter is on the upstream signal generated by the downstream transducer, we only implement the recovery angle on the downstream transducer by rotating it by about  $6^\circ$  in favor of the high flow velocity. Here,  $6^\circ$  is chosen as a compromise between high-flow and low-flow measurements.

### 2.3. Increasing SNR

Another method we use to increase the SNR is to electrically tune the transducer. This is common for transducer design, and has been abundantly discussed in literature and thus omitted here for conciseness.

### 2.4. Final Conceptual Design

The final conceptual design of our flare ultrasonic meter is schematically shown in Fig. 5 as a recap, where the center path length between transducers is kept relatively short, about 6", the path angle is chosen to be about  $45^\circ$ , and the  $6^\circ$  recovery angle is implemented to the downstream transducer only. Two carbon steel flowcells have been manufactured for prototyping and testing purposes based on the above conceptual design. One is called Bias 90 (refer to Fig. 6 (a)) where the two transducers are placed on the same side of the flowcell, and the other is called Diagonal 45 (refer to Fig. 6 (b)) where the two transducers are placed from two different sides of the flowcell. It should be emphasized that our transducers are rigidly mounted to avoid any problems with vibration due to high flow velocity by utilizing the specially-designed barrel assembly, and that testing has proven the ability to hold up to high velocity up to 120+m/s.

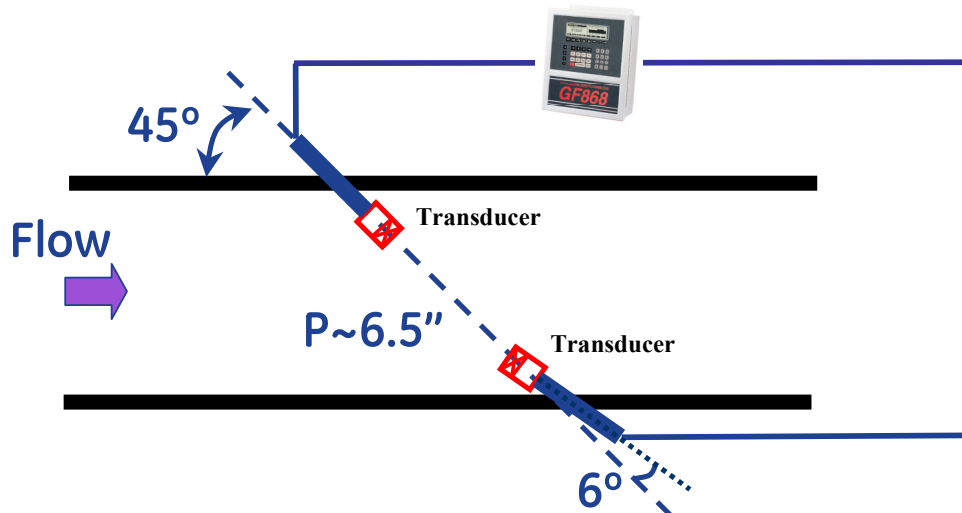


Fig. 5 Conceptual design of our flare gas ultrasonic flowmeter.

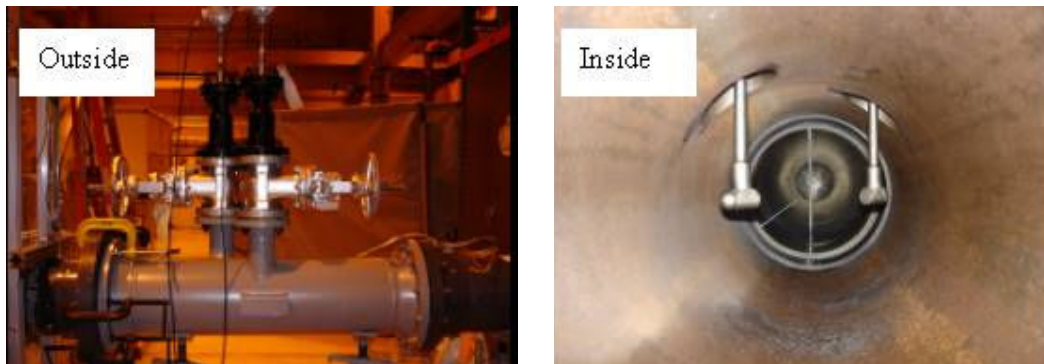


Fig. 6 (a) Pictures of the Bias 90 carbon steel flowcell with transducers mounted, outside and inside views.

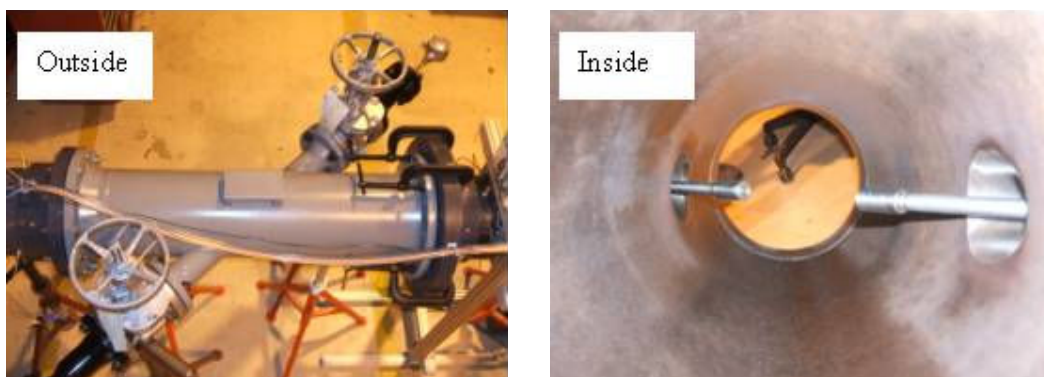


Fig. 6 (b) Pictures of the Diagonal 45 carbon steel flowcell with transducers mounted, outside and inside views.

### 3. Testing Facility

Flow testing was performed in the Energy and Propulsion Technologies Laboratory ([http://www.ge.com/research/grc\\_4\\_5.html](http://www.ge.com/research/grc_4_5.html)) at the GE Global Research Center (GRC) located in Niskayuna, NY in November, 2008. Fig.7 shows the overall layout of the testing facility. Air was supplied by an open circuit high mass flow system, which consists of a three stage centrifugal blower, capable of 0 to 20,000 scfm, with 16-inch piping and multiple control valves. An inline Venturi tube was utilized to measure the flow. The 16-inch piping gradually expands into a plenum, upon which the test apparatus is attached. Perforated screens inside the expansion and plenum ensure uniform flow.

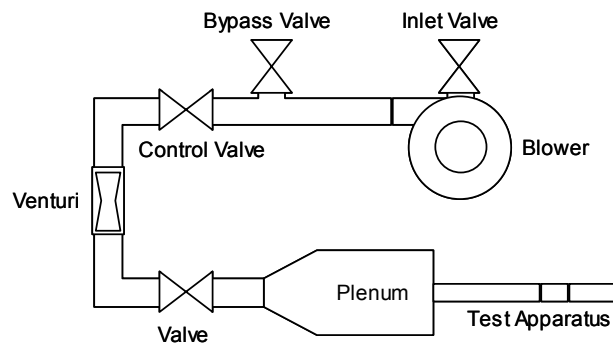


Fig. 7 Illustration of open flow system at GE GRC.

The test apparatus, schematically illustrated in Fig. 8, consisted of three sections; 1) a 10-inch Schedule 80 PVC pipe section, 10 times diameter in length upstream, 2) a 10-inch Schedule 40 carbon steel flow cell (~42 inch in length) in the middle, and 3) another 10-inch Schedule 80 PVC pipe section that is five times diameter in length downstream. The apparatus remained the same throughout the experiment with the exception of changing the flow cell to the alternate probe configurations. Fig. 9 shows a picture of the test apparatus for details.

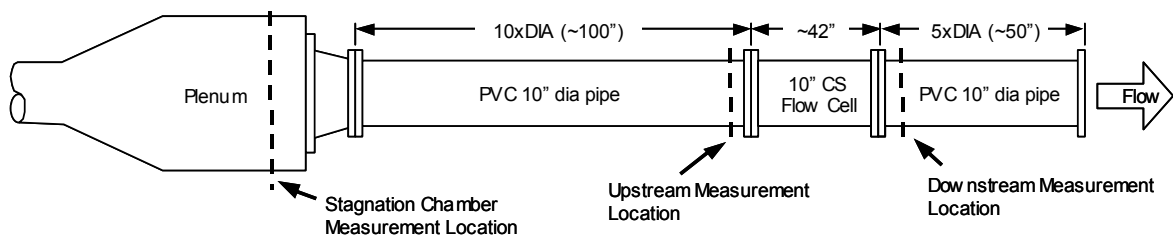


Fig. 8 Illustration of test apparatus with measurement locations.

Pressure and temperature measurements were made at four different locations; 1) the Venturi, 2) the plenum chamber, 3) upstream of the flow cell, and 4) downstream of the flow cell. The Venturi measurements were used to calculate mass flow and, in conjunction with local test-section measurements, the average velocity, which was used to set the reference velocity. The measurement location upstream of the flow cell was used to obtain the profile of the flow entering the flow cell. Total and static pressure measurements were made along this cross section of the pipe and were used to calculate the velocity profile using standard isentropic formula for one-dimensional flow.

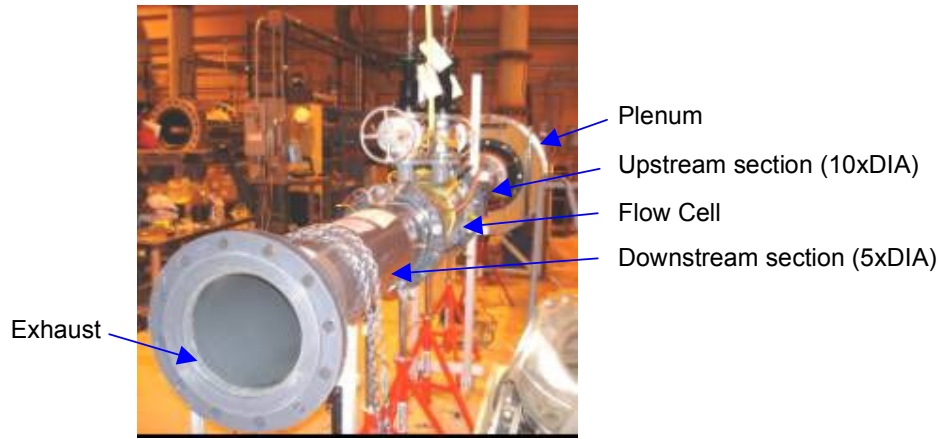


Fig.9 Picture of test apparatus.

#### 4. Test Results and Discussion

Fig. 10 (a) and Fig.10 (b) show the flow readings from our Flare meter (called GF868) in comparison with the GRC reference readings, for the Bias 90 configuration and the Diagonal 45 configuration, respectively. As seen our meter readings agree with the reference readings very well across the velocity range of 31.2 m/s up to 123.7 m/s. To analyze the results more quantitatively, we define the percentage error for our meter reading as follows:

$$\Omega(V) = \frac{Vm - Vref}{Vref} \times 100\%, \quad (9)$$

where  $Vm$  is our meter reading and  $Vref$  is the reference reading. Fig. 11 (a) and Fig. 11 (b) plot the percentage errors of our meter readings at different flow rates for the Bias 90 configuration and the Diagonal 45 configuration, respectively. The percentage errors for both Bias 90 and Diagonal 45 configurations are within 2% across the velocity range of 31.2 m/s up to 123.7 m/s. With the reference accuracy of 1-2% (dependent upon the flow velocity range, refer to Appendix for details), we can conclude that the overall meter accuracy is better than 3-4%.

In order to assess the repeatability of the new meter, we have defined the normalized standard deviations of our meter readings at a given flow as follows:

$$\mathfrak{R} = \frac{\sigma(Vm)}{Vm}, \quad (10)$$

where  $\sigma(Vm)$  is the standard deviation of our meter measurements,  $Vm$ , over a typical five-minute period. Fig.12 (a) and Fig.12 (b) show the relative standard deviation of our meter at different flowrates, for Bias 90 and Diagonal 45 configurations, respectively. As shown, the relative standard deviation of our meter is less than 1.2% for all the testing points. However, it should be noted that the relative standard deviation is increasing with flow velocity in general. This is due to the higher uncertainty at higher flow rates, causing more turbulence, beam drift, signal distortion, flow noise and eventually lower SNR.

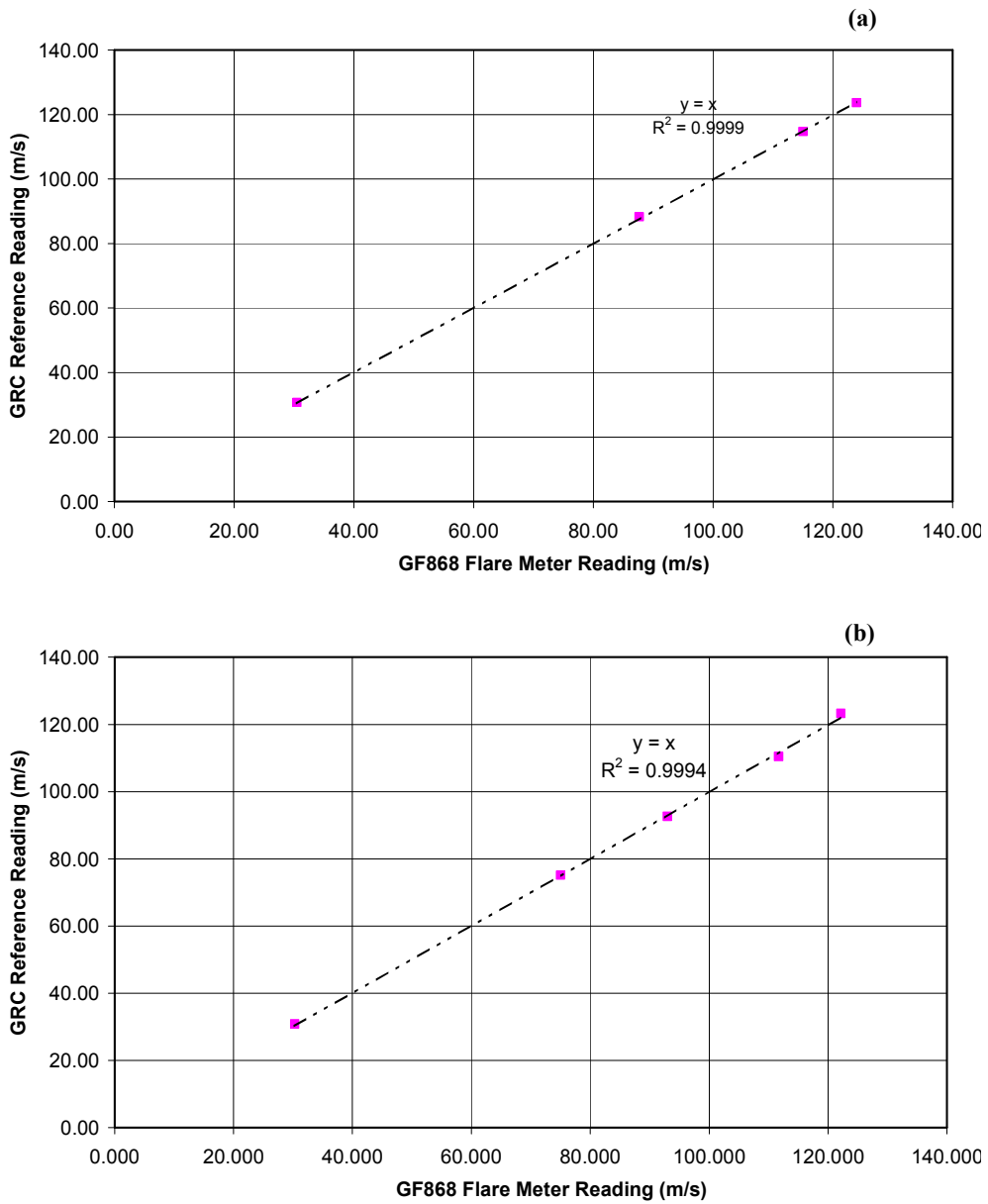


Fig. 10 (a) GE GF868 flare meter reading in comparison with GRC reference reading for the Bias 90 configuration; (b) GE GF868 flare meter reading in comparison with GRC reference reading for the Diagonal 45 configuration.

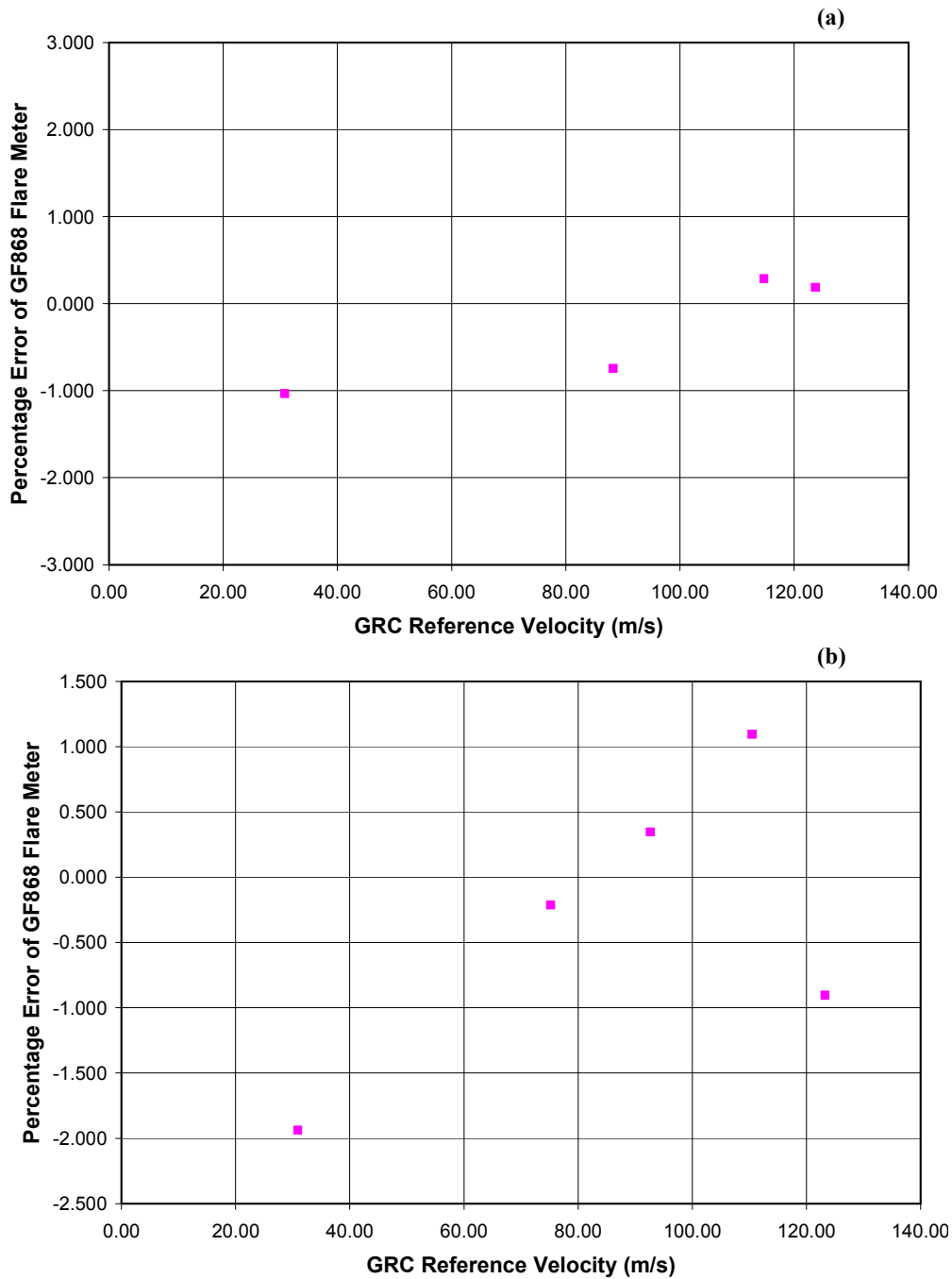


Fig. 11 (a) The percentage error of GE GF868 flare meter readings for the Bias 90 configuration; (b) The percentage error of GE GF868 flare meter readings for the Diagonal 45 configuration.

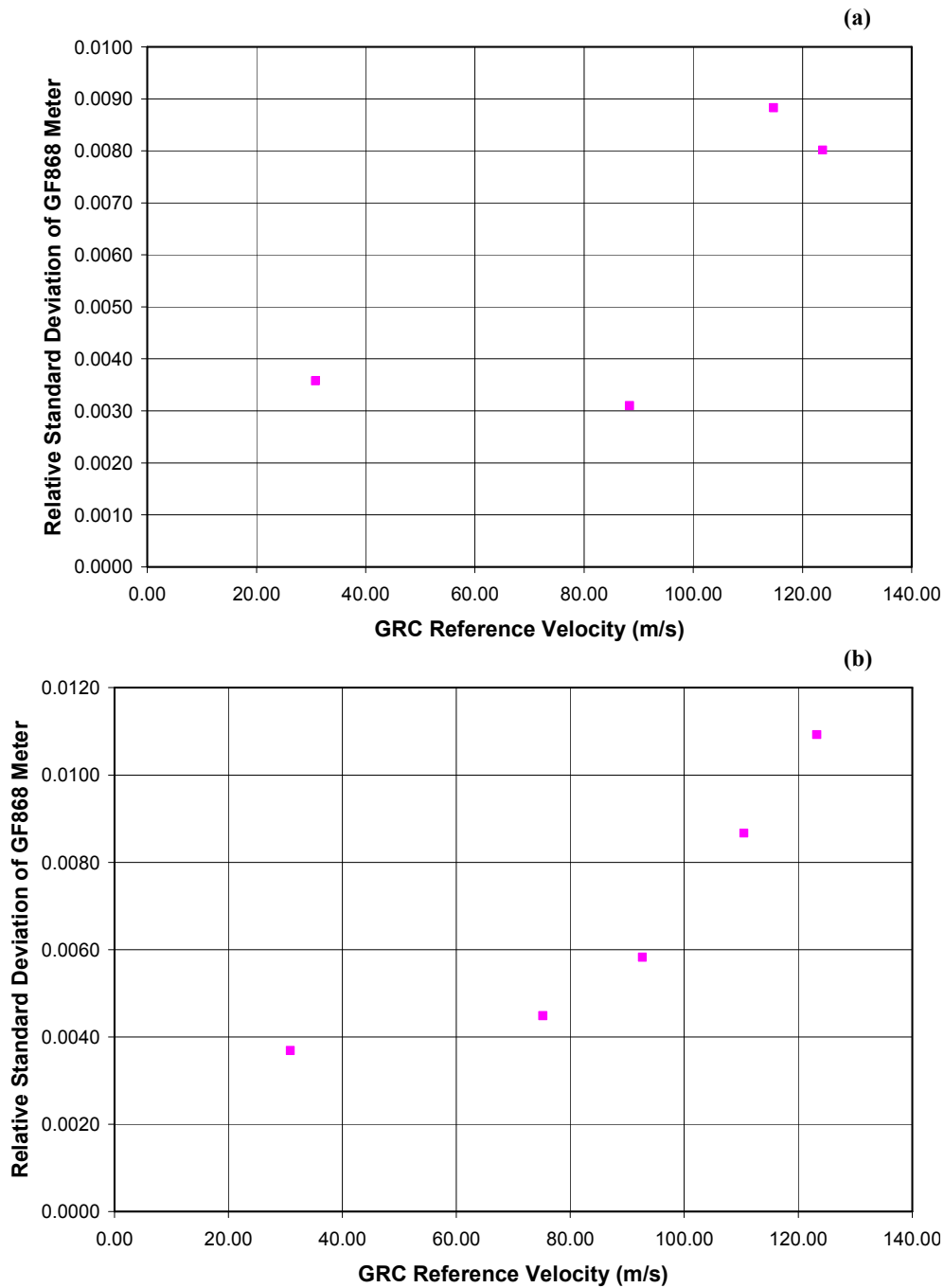
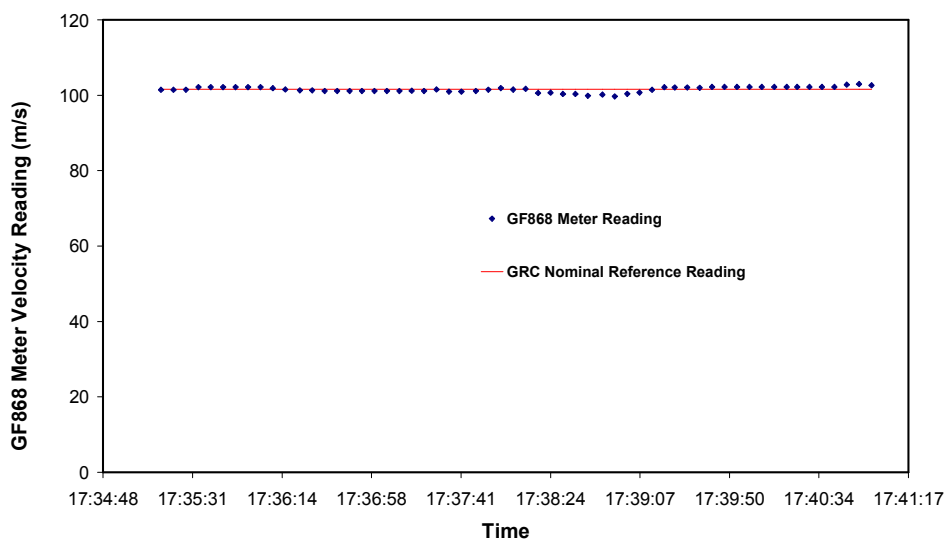


Fig. 12 (a) Relative standard deviation of GE GF868 meter reading for the Bias 90 configuration; (b) Relative standard deviation of GE GF868 meter reading for the Diagonal 45 configuration.

To test the relationship between path length and maximum measurable flow rate, we increase the path length from 6.5" to 14", making the transducer non-intrusive to the flow for the 10-inch flowcell. Fig. 13 shows the log of the measurements at 101.56 m/s for about 5 minutes. The meter readings are consistent and reliable. However, the 14-inch separation does not allow us to reliably measure air flow of 120 m/s or above. As expected, a compromise has to be made between the maximum measurable flow rate and the path length. For example, a shorter path, say 6", could lead to a maximum measurable flow rate of 125 m/s, using a simple linear interpolation based on the above two testing points (i.e., 6.5" and 14" transducer separations give the maximum measurable flow rates of 123.7 m/s and 101.56 m/s, respectively.).



*Fig. 13 Time log of GE GF868 meter reading compared to nominal GRC reference reading of 101.56 m/s for the 14-inch transducer separation of the Diagonal 45 configuration.*

It has to be stressed that all the tests we have done in this paper are in air at roughly room temperature. In real flare application, depending on gas composition, the maximum measurable flow rate could be larger than the limit demonstrated above in air, particularly because the beam drift angle is Mach number dependent. In other words, a flare gas with a higher speed of sound will result in a lower Mach number and thus a smaller beam drift angle, which in return would potentially allow for measuring higher flow velocity.

## 5. Conclusion

In summary, for the first time, an ultrasonic flare gas flow meter has been developed to demonstrate the accurate measurement of air flow up to 123.7 m/s. Some of the new enabling technologies are detailed, primarily focused on the mechanical and transducer developments. Testing data have been presented for two typical configurations, Bias 90 and Diagonal 45, in comparison with a Venturi reference. The overall accuracy of our meter is shown to be better than 3-4% with reference meter uncertainty included, dependent upon the flow velocity range, and the relative standard deviation of our meter readings is within 1.2%. The new development

could potentially translate into an even higher flow-velocity flare gas measurement, depending on the flare gas composition.

### **Appendix: GRC Reference Uncertainty**

All pressure and temperature measurements were made using National Institute of Standards and Technology (NIST) traceable instrumentation. At each velocity set point, a time delay preceded sampling to ensure flow stabilization. Each sensor would then be sampled for 10 seconds, at 10 measurements per second, and averaged for that point; this procedure was followed for all measurements. Each sensor was calibrated by NIST traceable calibration equipment prior to testing, in addition to manufacturer calibration. The uncertainty in the measurements varied by sensor type. For the static pressure sensors, the combined uncertainty,  $u_c$ , was  $\pm 51.74$  Pa, while the total pressure sensor  $u_c$  was  $\pm 51.97$  Pa. The Venturi measurement used pressure sensors with the upstream  $u_c$  equal to  $\pm 89.69$  Pa and the throat  $u_c$  equal to  $\pm 35.23$  Pa. The temperature sensors used were standard type T thermocouples. The  $u_c$  values for the Venturi, stagnation chamber, and test section temperatures were  $\pm 0.41$  K,  $\pm 0.42$  K, and  $\pm 0.41$  K, respectively. The technique used to determine measurement uncertainty for the instrumentation is outlined in NIST Technical Note 1297<sup>[16]</sup>.

The  $u_c$  values were conservatively propagated through the velocity calculations for each measurement, and therefore varied at each velocity point. Typical velocity error for the profile measurements is less than 1.0%, with higher error values at the low velocities ( $\leq 50$  m/sec). Typical error for the reference velocity measurements is less than 2.0%, with higher error values at the low velocities ( $\leq 50$  m/sec). For example in uncertainty; the free stream velocity value of 120.6 m/sec  $\pm 0.8$  m/sec, and the reference velocity of 112.5 m/sec  $\pm 1.8$  m/sec.

### **Acknowledgment**

The authors acknowledge William Hunt at GE—Sensing for his help with the recovery angle drafting, Kevin Shufon and Matthew Boespflug at GE Global Research Center for their support with the flow tests, and Kimberly Lord at GE—Sensing for her help with some of the illustrations. In addition, the authors acknowledge Oleg Khrakovsky, Nicholas J. Mollo, James Korba, Keith Coleman and David Martin at GE—Sensing for their help with some of the tests, the GF868 meter electronics and signal processing. Special thanks are due to Daryl Belock, Christopher Brolin, John Luff, Shirley Ao, Ashish Bhandari and Ted Furlong at GE—Sensing for their support, interest and comments.

**References:**

- [1] J.W. Smalling, L.D. Braswell, L.C. Lynnworth, and D.R. Wallace, Flare Gas Ultrasonic Flow Meter, Proceedings from the Thirty-Ninth Annual Symposium on Instrumentation for the Process Industries, pp. 27-38, 1984.
- [2] D. Belock, How much do you flare?—How to measure flowrates of flare gas accurately and reliably, Process worldwide, Issue 3, pp. 18-19, 2006.
- [3] NORWEGIAN PETROLEUM DIRECTORATE. Regulations to measurement of fuel and flare gas for calculation of CO<sub>2</sub> tax in the petroleum activities, August 1993 (ISBN 82-7257-395-4).
- [4] L. Sui and T.H. Nguyen, Ultrasonic Flow Meter, US Patent No. 7658114, 2010.
- [5] K.S. Mylvaganam, High-rangeability ultrasonic gas flowmeter for monitoring flare gas, IEEE Transactions on Ultrasonics, Ferroelectrics and Frequency Control, Vol. 36, pp. 144-149, 1989.
- [6] GE Sensing GF868 Brochure, [http://www.gesensing.com/downloads/datasheets/920\\_009c.pdf](http://www.gesensing.com/downloads/datasheets/920_009c.pdf)
- [7] O. Rutten, Deutsches Patent No. 520484, 1928.
- [8] L.C. Lynnworth, Ultrasonic Measurement for Process Control: Theory, Techniques, Applications, Academic Press, 1989.
- [9] ANSI/ASME MFC-5M-1985, “Measurement of Liquid Flow in Closed Conduits Using Transit-Time Ultrasonic Flowmeters”, An American National Standard, 1994.
- [10] M.F. Hamilton and D.T. Blackstock, Nonlinear Acoustics: Theory and Application, Academic Press, 1998.
- [11] L.E. Kinsler, A.R. Frey, A.B. Coppens and J.V. Sanders, Fundamentals of Acoustics, John Wiley & Sons, 3<sup>rd</sup> Ed., pp. 179, 1982.
- [12] FUNDAMENTALS OF ELECTROACOUSTICS, <http://www.massa.com/fundamentals.htm>
- [13] L.C. Lynnworth, D.R. Patch and W.C. Mellish, “Impedance-Matched Metallurgically Sealed Transducer, IEEE Transactions on Sonics and Ultrasonics, Vol. SU-31, pp. 101-104, 1984.
- [14] J. Krautkramer and H. Krautkramer, Ultrasonic Testing of Materials, Springer-Verlag, 4<sup>th</sup> Ed., pp. 73, 1990.
- [15] P.M. Morse and K.U. Ingard, Theoretical Acoustics, Chapter 11, Princeton, 1986.
- [16] B.N. Taylor and C.E. Kuyatt, *Guidelines for Evaluating and Expressing the Uncertainty of NIST Measurement Results*, NIST Technical Note 1297, 1994.